

Color shift reduction of a multi-domain IPS-LCD using RGB-LED backlight

Ruibo Lu, Qi Hong, Zhibing Ge, and Shin-Tson Wu

College of Optics and Photonics, University of Central Florida, FL 32816

swu@creol.ucf.edu

Abstract: Color gamut and static and dynamic color shifts of a multi-domain in-plane-switching liquid crystal display (IPS LCD) are calculated quantitatively using RGB (red, green, and blue) light-emitting diodes (LEDs) and cold-cathode fluorescent lamp (CCFL) backlights. Simulation results indicate that the LED backlight exhibits a wider color gamut, better angular color uniformity, and 2-4X smaller static and dynamic color shifts than the CCFL system.

©2006 Optical Society of America

OCIS codes: (230.3720) Liquid crystal devices; (330.1690) Color

References and Links

1. G. Harbers and C. Hoelen, "High performance LCD backlight using high intensity red, green and blue light emitting diodes," Soc. Inf. Display Tech. Digest **32**, 702-705 (2001).
2. R. West, H. Konijn, W. Silevis-Smitt, S. Kuppens, N. Pfeffer, Y. Martynov, Y. Takaaki, S. Eberle, G. Harbers, T. Tan, and C. Chan, "High brightness direct LED backlight for LCD-TV," Soc. Inf. Display Tech. Digest **34**, 1262-1265 (2003).
3. H. Hsieh, C. Chou, and W. Li, "Vivid color and clear motion picture 32-inch TFT-LCD TV with scan RGB LED backlight," Proc. Int'l Display Manufacturing Conf. pp. 622-644 (2005).
4. A. Konno, Y. Yamamoto, and T. Inuzuka, "RGB color control system for LED backlight in IPS-LCD TVs," Soc. Inf. Display Tech. Digest **36**, 1380-1383 (2005).
5. W. Kim, "Technology overview: LCDs for TV application," J. SID **12**, 449-453 (2004).
6. S. Aratani, H. Klausmann, M. Oh-e, M. Ohta, K. Ashizawa, K. Yanagawa, and K. Kondo, "Complete suppression of color shift in in-plane switching mode liquid crystal displays with a multidomain structure obtained by unidirectional rubbing," Jpn. J. Appl. Phys. **36**, L27-L29 (1997).
7. H. Klausmann, S. Aratani, and K. Kondo, "Optical characterization of the in-plane switching effect utilizing multidomain structures," J. Appl. Phys. **83**, 1854-1862 (1998).
8. R. Lu, X. Zhu, S. T. Wu, Q. Hong, and T. X. Wu, "Ultrawide-view liquid crystal displays," J. Display Technology **1**, 3-14 (2005).
9. M. Fairchild, *Color Appearance Models (2nd Edition)*, (Wiley, New York, 2005).
10. F. Bunting, *Color Primer -- An Introduction to the History of Color, Color Theory, and Color Measurement*, (Light Source Computer Images, Inc., 1998).
11. N. Ohta and A. Robertson, *Colorimetry -- Fundamentals and Applications*, (Wiley, New York, 2005).
12. G. Wyszecki and W. Stiles, *Color Science -- Concepts and Methods, Quantitative Data and Formulate (2nd Edition)*, (Wiley, New York, 1982).
13. R. Hunt, *Measuring Colour (2nd Edition)*, (Ellis Horwood, West Sussex, 1991).
14. S. T. Wu, "Birefringence dispersion of liquid crystals", Phys. Rev. **A33**, 1270-1274 (1986).
15. R. Lu, S. T. Wu, Z. Ge, Q. Hong, and T. X. Wu, "Bending angle effects on the multi-domain in-plane-switching liquid crystal displays," J. Display Technology **1**, 207-216 (2005).
16. A. Lien, "A detailed derivation of extended Jones matrix representation for twisted nematic liquid crystal displays," Liq. Cryst. **22**, 171-175 (1997).
17. P. Downen, "A closer look at flat-panel-display measurement standards and trends," Information Display **22**, 16-21 (2006).

1. Introduction

The use of light emitting diode (LED) array as a backlight unit for liquid crystal displays (LCDs) is emerging rapidly in cell phones, computer monitors, and televisions. LED offers tremendous performance advantages over the conventional cold-cathode fluorescent lamp

(CCFL) in larger color gamut, higher brightness, tunable backlight white point control by separate red, green and blue (RGB) colors, real-time color management, reduced motion artifacts without brightness and lifetime penalty, and higher dimming ratio [1-4].

For high-end LCD monitors and TVs, small color shift, fast response time, wide viewing angle, high contrast ratio, and high optical efficiency are the major technical challenges [5]. To achieve these goals, the multi-domain in-plane-switching (IPS) LCD has been developed [6, 7, 8]. Such multi-domain IPS LCD provides a reduced color shift under the white CCFL backlight at obliquely incident angle [7, 8].

Although the LED advantages are realized, but so far no quantitative results have been reported in detail. In this paper, we compare the color gamut and static and dynamic color shifts of a multi-domain IPS LCD using LED and CCFL backlights. The static color shift is particularly important for LCD monitors while dynamic color shift is crucial for LCD TVs.

2. Modeling of color shift

In the history of color science, several approaches and models have been developed to analyze the displayed color images [9, 10, 11]. Typically, they are divided into two groups. The first approach is the spectral method which measures the wavelength composition of the light that leaves the display panel. This method provides an absolute description of the color properties of an object such as how it emits, reflects, or transmits at different wavelengths in the visible spectral range. The second approach is the tristimulus method which is basically a three-valued system that models the appearance of color by human eye. This method, established and developed by the Commission International de l'Éclairage (CIE) [12], needs to include the specifications of the observer, light source, device, and other aspects of the viewing conditions.

2.1 Tristimulus values and chromaticity coordinates for CIE 1931

The CIE XYZ color space defines all the colors in terms of three imaginary primaries X, Y, and Z based on the human visual system. The X, Y, Z tristimulus values of a colour stimulus ($S(\lambda)$) which represent the luminance or lightness of the colors are expressed as

$$X = k \int_{380 \text{ nm}}^{780 \text{ nm}} S(\lambda) \bar{x}(\lambda) d\lambda, \quad Y = k \int_{380 \text{ nm}}^{780 \text{ nm}} S(\lambda) \bar{y}(\lambda) d\lambda, \quad Z = k \int_{380 \text{ nm}}^{780 \text{ nm}} S(\lambda) \bar{z}(\lambda) d\lambda \quad (1)$$

Here, the values of $\bar{x}(\lambda)$, $\bar{y}(\lambda)$, and $\bar{z}(\lambda)$ color matching functions are the tristimulus values of the monochromatic stimuli, $S(\lambda)$ represents the spectral radiometric quantity at a certain wavelength λ , e.g., it is the light transmission intensity in a practical LCD device, and k is a constant [12].

Since the X, Y, and Z tristimulus values are not easy to interpret so that it is difficult to tell what the color they specify, the chromaticity coordinates x , y , z have been introduced by CIE in the following forms:

$$x = \frac{X}{X + Y + Z}, \quad y = \frac{Y}{X + Y + Z}, \quad z = \frac{Z}{X + Y + Z} \quad (2)$$

Because $x + y + z = 1$, it is sufficient to just use two chromaticity coordinates to describe the chromaticity of the stimulus. That means x and y can be plotted in a two-dimensional graph containing all the color information of the original X, Y, and Z values. The corresponding chromaticity diagram is referred as CIE 1931 diagram which is the first standard colorimetric system including the color matching functions for the standard observer, standard illuminants, and standard light sources [13].

2.2 CIE 1976 uniform chromaticity scale (UCS) diagram

To obtain the reasonably equidistant chromaticity scales that are better than the CIE 1931 diagram, the CIE 1976 uniform chromaticity scale (UCS) diagram which is also called (u' , v') diagram has been introduced. The (u' , v') coordinates are related to the (x , y) coordinates by the following equations:

$$u' = \frac{4X}{X + 15Y + 3Z} = \frac{4x}{-2x + 12y + 3}$$
$$v' = \frac{9Y}{X + 15Y + 3Z} = \frac{9y}{-2x + 12y + 3}$$
(3)

2.3 Color shift based on CIE color difference equations

Color shift is an important parameter to determine the color uniformity of a LCD panel. The angular-dependent color uniformity of a LCD monitor is usually measured by a spectroradiometer with capacity of presenting u' and v' coordinates when the monitor color is set at the full-bright state. The chromaticity coordinates u' and v' are measured in the visually most color deviating areas such as the horizontal and vertical directions of a LCD panel.

Based on Eq. (3), $\Delta u'v'$ at any two positions (1 and 2) can be calculated using the following formula

$$\Delta u'v' = \sqrt{(u'_2 - u'_1)^2 + (v'_2 - v'_1)^2} .$$
(4)

For LCD monitors, $[u'_2, v'_2]$ represent the $[u', v']$ values at an oblique viewing angle while $[u'_1, v'_1]$ are usually referred to the $[u', v']$ values at normal viewing angle. For LCD TVs, the color difference between different gray scales becomes much more important than that of the static evaluation of a LCD monitor. Therefore, the $[u'_2, v'_2]$ and $[u'_1, v'_1]$ values for a LCD TV should represent the $[u', v']$ values at different gray levels.

In the following sections, we will evaluate the static and dynamic color shifts of a multi-domain IPS-LCD using RGB-LED and CCFL backlights. The static color shift is referred to the full-bright state, i.e., 255th gray level (G255) and the dynamic one is based on the color difference from 63rd gray (G63) to G255.

3. IPS-LCD device and simulation approaches

3.1 Device structure and working principle

Figure 1 shows the device structure and its working principle of the simulated multi-domain IPS LCD. Both positive and negative dielectric anisotropy ($\Delta\epsilon$) LC materials can be used. In Fig. 1(a), the rubbing direction is set along the vertical direction and the LC directors are aligned homogeneously on the glass substrates. The chevron-shaped electrode has a bending angle, α , which is set as the angle between the chevron arm extension direction and the vertical direction. A series of chevron-shaped electrodes are alternatively arranged to form the inter-digital electrodes on the same substrate as the common electrode and the pixel electrode, respectively, which are connected to the thin-film transistors in a practical LCD device.

In Fig. 1(b), the transmission axis of the linear polarizer near the bottom substrate is parallel to the LC alignment (i.e., rubbing) direction. When there is no voltage applied, the incident light is completely blocked by the crossed polarizers, which results in a normally black state. When the applied voltage exceeds the Freedericksz transition threshold, the transversal electric fields between the electrodes, shown as parabolic lines, are able to reorient the LC directors. The LC material with positive (or negative) $\Delta\epsilon$ between the electrodes would be reoriented along (or perpendicular) the electric field direction. The LC directors above the

two chevron arm regions are twisted into opposite directions so that the multi-domain LC configuration is generated and light transmits through the crossed polarizers.

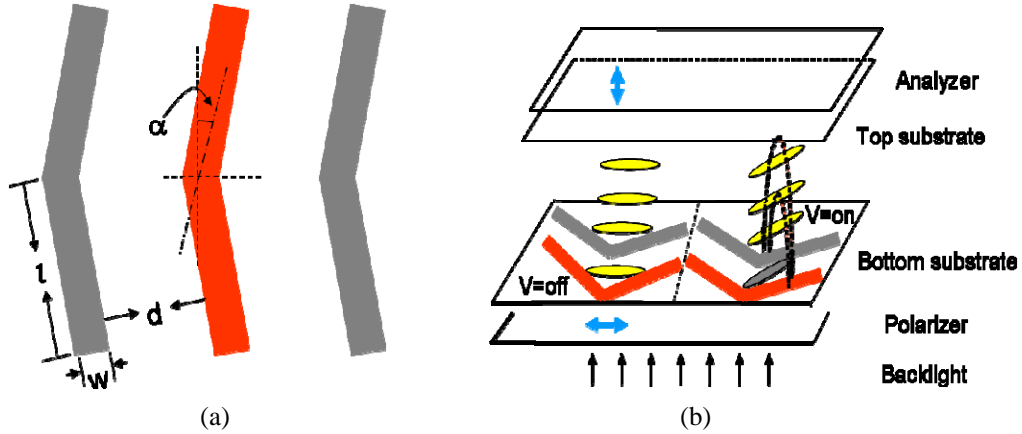


Fig. 1. (a) The electrode structure and (b) the working principle of the multi-domain IPS-LCD.

As an example, we simulate a chevron-shaped multi-domain IPS LCD using a Merck positive LC material MLC-6692. Its physical properties are summarized as follows: $\gamma_1=0.1$ Pa·s, $\Delta\epsilon=10.3$, $K_{11}= 9.6$ pN, $K_{22}= 6.1$ pN, $K_{33}= 14.1$ pN, and $\Delta n=0.085$ at $\lambda= 550$ nm. The birefringence dispersion [14] of the LC material at each wavelength of the light source is included in the calculation using the following equation:

$$\Delta n = G \cdot \frac{\lambda^2 \cdot \lambda^{*2}}{\lambda^2 - \lambda^{*2}} \quad (5)$$

At room temperature, the two fitting parameters are: $G= 1.646 \times 10^{-6} \text{ nm}^{-2}$ and $\lambda^{*2}=210$ nm. In our design, the cell gap is $d=4 \mu\text{m}$, the width of the chevron-shaped electrode is $w= 3 \mu\text{m}$, the electrode gap is $g= 8 \mu\text{m}$, and the chevron arm length is $l= 128 \mu\text{m}$. The bending angle of the chevron-shaped electrodes, α , is typically chosen at 10° , and LC pretilt angle is 2° with respect to the substrate plane.

3.2 Simulation approaches and optical calculations

The simulation sequence is to obtain the dynamic 3-D LC director distributions first and then calculate the detailed electro-optics of the LCD. We have developed a 3-D simulator for calculating the LC director distributions, which combines the finite element method and finite difference method approaches to improve the calculation speed [15]. Once the LC director distribution profiles are obtained, we then calculate the electro-optic properties of the LCD using the extended Jones matrix method [16]. The LC layer is modeled as a stack of uniaxial homogeneous layers. Here, we assume the reflections between the interfaces are negligible. Therefore, the transmitted electric field is related to the incident electric field by

$$\begin{bmatrix} E_x \\ E_y \end{bmatrix}_{N+1} = \mathbf{J} \begin{bmatrix} E_x \\ E_y \end{bmatrix}_1 = \mathbf{J}_{Ext} \mathbf{J}_N \mathbf{J}_{N-1} \cdots \mathbf{J}_2 \mathbf{J}_1 \mathbf{J}_{Ent} \begin{bmatrix} E_x \\ E_y \end{bmatrix}_1, \quad (6)$$

where \mathbf{J}_{Ext} and \mathbf{J}_{Ent} are the correction matrices considering the transmission losses in the air-LCD interface, which are given by

$$\mathbf{J}_{Ent} = \begin{bmatrix} \frac{2 \cos \theta_p}{\cos \theta_p + n_p \cos \theta_k} & 0 \\ 0 & \frac{2 \cos \theta_k}{\cos \theta_k + n_p \cos \theta_p} \end{bmatrix}, \quad (7a)$$

$$\mathbf{J}_{Ext} = \begin{bmatrix} \frac{2n_p \cos \theta_k}{\cos \theta_p + n_p \cos \theta_k} & 0 \\ 0 & \frac{2n_p \cos \theta_p}{\cos \theta_k + n_p \cos \theta_p} \end{bmatrix}. \quad (7b)$$

Correspondingly, the overall optical transmittance is represented as

$$t_{op} = \frac{|E_{x,N+1}|^2 + \cos^2(\theta_p)|E_{y,N+1}|^2}{|E_{x,1}|^2 + \cos^2(\theta_p)|E_{y,1}|^2}, \quad (8)$$

where θ_p is given by

$$\theta_p = \sin^{-1}(\sin(\theta_k) / \text{Re}(n_p)). \quad (9)$$

Here, n_p is the average refractive index of the polarizer, where $n_p = (2n_{e,p} + n_{o,p})/3$, $n_{e,p} = 1.500 + i \times 3.251 \times 10^{-3}$ and $n_{o,p} = 1.500 + i \times 2.86 \times 10^{-5}$, $\text{Re}(n_p)$ stands for the real part of n_p , and θ_k is the azimuthal angle of the incident wavevector \mathbf{k} .

4. Results and discussion

4.1 LC director distribution and voltage-dependent transmittance curve

Figure 2 plots the typical LC directors distribution in the central layer of a multi-domain IPS LC cell at $\alpha=10^\circ$ and $V=5.0 \text{ V}_{\text{rms}}$. It is clearly shown that the LC directors are twisted into different directions in-between the neighboring electrodes; especially, the LC directors on the two chevron arm regions are switched into complementary directions. Therefore, the chevron-shaped electrodes help to form four-domain LC configurations.

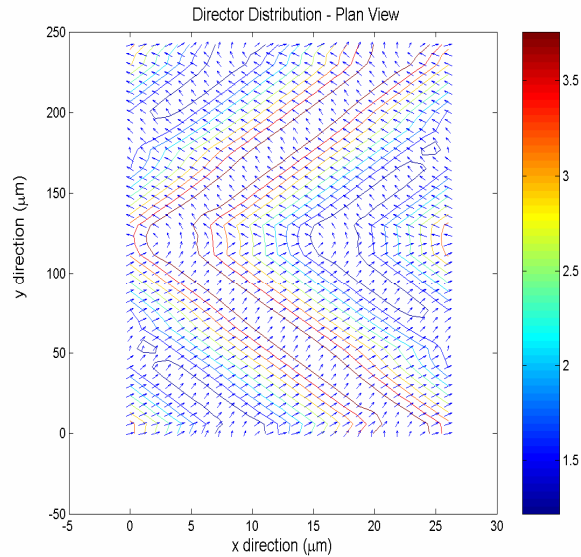


Fig. 2. Typical director distribution of the multi-domain IPS-LCD in the central layer.

Figure 3 shows the voltage-dependent transmittance (VT) curve of the multi-domain IPS LCD at the selected three primary colors (R=650, G=550, and B=450 nm), where the polarizer and analyzer pair has a maximum transmittance of 35%. The birefringence dispersion of MLC-6692 as described in Eq. (5) has been taken into consideration. At $V = 5.0 V_{rms}$, RGB primaries all reach their respective maximum transmittance, which is the full-bright gray level G255. The gray level G63 is at the position of the one fourth of the maximum transmittance, where the operation voltage is $3.25 V_{rms}$. In the following part, we will calculate the color shifts at different gray levels based on their corresponding voltages.

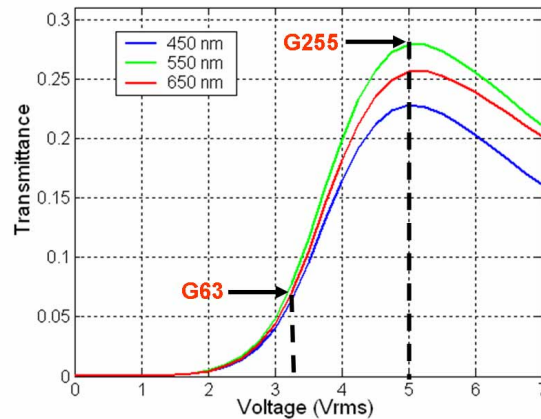


Fig. 3. VT curve of the multi-domain IPS LCD at R=650, G=550, and B=450 nm.

4.2 Color gamut of IPS-LCD panel under LED and CCFL backlights

The gamut of a device is referred to the range of colors that it can reproduce or distinguish. For a LCD device such as a monitor or a TV panel, its gamut can be plotted with the device's RGB primaries. This is one of the most common uses for the CIE diagram, especially in the gamut comparisons.

Figure 4(a) shows the typical backlight spectra of RGB LEDs. The red LED (AlInGaP) has a peak wavelength at $R \sim 630$ nm and a full-width-half maximum FWHM ~ 22 nm, the

green LED (InGaN) has a peak wavelength at $G \sim 535$ nm and $FWHM \sim 43$ nm, and the blue LED (InGaN) has a peak wavelength at $B \sim 460$ nm and $FWHM \sim 24$ nm [1]. Figure 4(b) shows the typical transmission spectra of the CCFL through the RGB color filters (for simplicity, let us call them CCFL primaries). They have the average peak wavelengths at $R \sim 650$ nm, $G \sim 550$ nm and $B \sim 450$ nm. Their respective bandwidth is much wider than that of LED primaries.

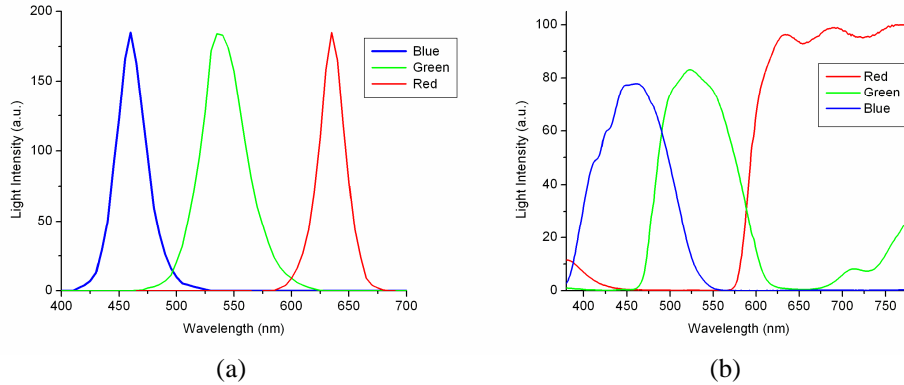


Fig. 4. (a) RGB backlight spectra of LEDs and (b) the color filter spectra from CCFL.

Figure 5 plots the RGB primaries through the IPS LCD panel using LED and CCFL backlights. The color gamut defined by the RGB-LED color points in the color diagram is larger than that of the CCFL primaries and the National Television System Committee (NTSC) standard primaries. It means that it is possible to obtain a more than 100% NTSC color gamut by properly selecting the LED colors and the color filters. Meanwhile, the color gamut achieved by the CCFL backlight is much narrower than that of LED backlight or NTSC standard. In a LCD using CCFL backlight, the color gamut is only 65-75% of the NTSC standard. The reduced color gamut mainly results from the wide bandwidth of the employed RGB color filters. As shown in Fig. 4(b), there is an evident green light leakage through the blue color filters. In principle, we can design narrow band color filters to improve the color purity, but the optical efficiency will be sacrificed. The RGB LED spectra are narrow and they have a very little overlap. Therefore, their color gamut exceeds the NTSC standard.

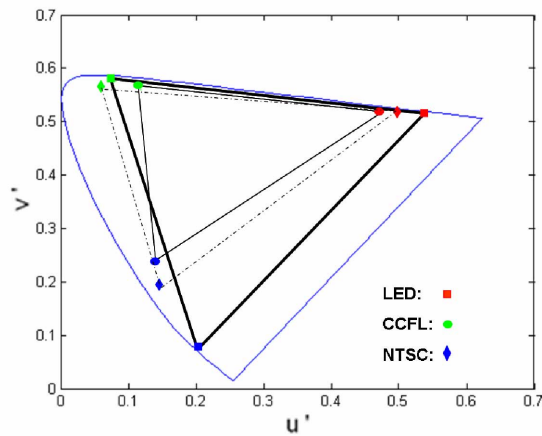


Fig. 5. The RGB primaries through IPS-LCD panel for LED and CCFL backlights and NTSC standard primaries on the CIE 1976 UCS diagram.

4.3 Static color shift for RGB primaries at the set incident angle

Figure 6 compares the static color shift of the multi-domain IPS LCD at the full-bright gray level G255 ($V=5 V_{rms}$) for LED and CCFL backlights. The incident angle of the RGB primaries is fixed at 60° from the normal of the LCD panel. They are then scanned across the whole 360° azimuthal angle (ϕ) at 10° scanning step. Both CCFL and LED RGB primaries show very small color shift in the CIE 1976 UCS ($u'v'$) color diagram. The reason for the small color shift in the multi-domain IPS mode originates from that the LC directors are reoriented into complementary directions in each sub-domain as shown in Fig. 2 [15].

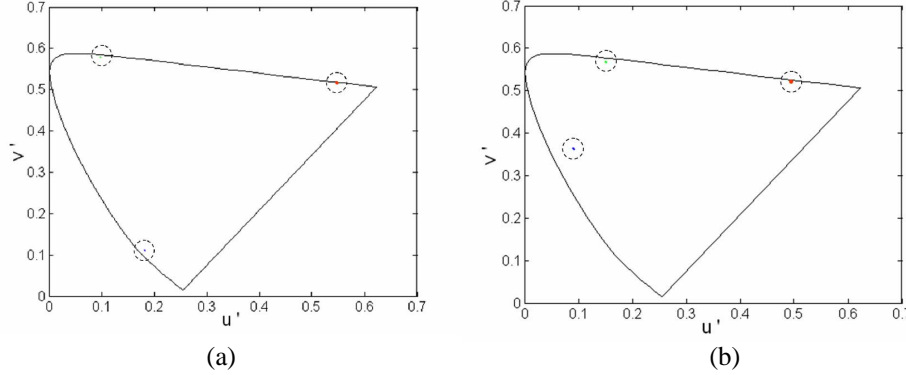


Fig. 6. Static color shift for RGB primaries at 60° incident angle: (a) LED and (b) CCFL.

4.4 Static color shift for RGB primaries at different incident angles

As shown in Figure 7, we further plot the CIE 1976 UCS diagrams with different incident angles at the full-bright gray level G255 ($V=5 V_{rms}$) for LED and CCFL backlights. The incident angle is defined as the angle between the light incident direction and the normal of the LCD panel, which is referred as theta angle θ thereafter. In our calculations, we vary the theta angle from -80° to 80° . It is evident that the LED-lit LCD has a much weaker color shift than CCFL in all the RGB primaries.

Besides color gamut, angular color uniformity is another important consideration. To investigate angular color uniformity, we redefine Eq. (4) as

$$\Delta u'v' = \sqrt{(u'_{\max} - u'_{\min})^2 + (v'_{\max} - v'_{\min})^2}, \quad (10)$$

where $[u'_{\max}, v'_{\max}]$ and $[u'_{\min}, v'_{\min}]$ represent the maximum and minimum $[u', v']$ values at the full-bright state between $0-80^\circ$ viewing range. For the multi-domain IPS LCD, we obtain $\Delta u'v' = (0.0083, 0.0246, 0.0403)$ for LED and $\Delta u'v' = (0.0299, 0.0491, 0.1569)$ for CCFL backlight at the RGB primaries. Therefore, the LED IPS-LCD shows a $\sim 2-3X$ better angular color uniformity than the conventional CCFL IPS-LCD.

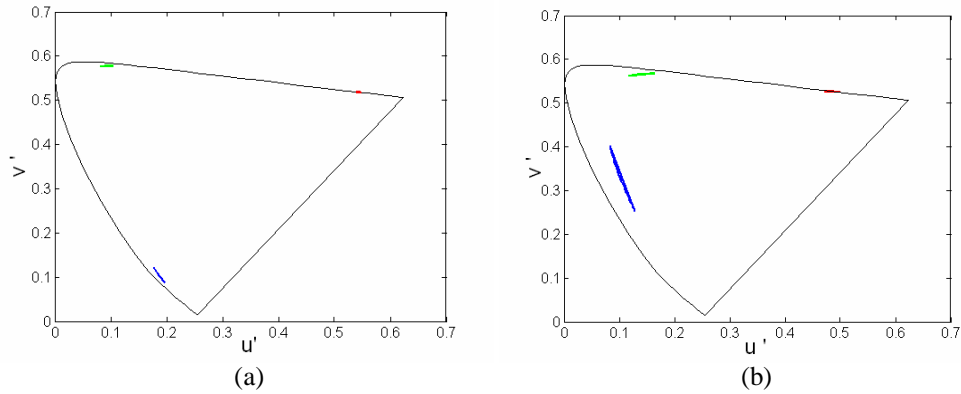


Fig. 7. Static color shift for RGB primaries at the varied incident angles from 0° to 80° : (a) LED and (b) CCFL.

4.5 Static color shift in the horizontal and vertical directions

In evaluating the color uniformity of a LCD monitor, the observers care more about the color performance in the horizontal and vertical directions. The color shifts in these two directions are usually reported experimentally [5, 17]. Figures 8(a) and 8(b) show the simulated angular dependent $\Delta u'v'$ of the LED- and CCFL-lit IPS LCDs as observed from the horizontal ($\phi=0^\circ$) and vertical ($\phi=90^\circ$) viewing directions. For both lighting systems, the RGB curves are fairly symmetric. A slightly larger deviation is observed for the blue primary when θ is larger than 50° . This symmetric behavior is attributed to the symmetric LC domain formations in both horizontal and vertical directions under the transverse electric field as Fig. 2 shows. However, in both LED and CCFL backlit IPS-LCDs, blue color has the largest $\Delta u'v'$ value, and then followed by green and red. As expected, the LED system exhibits a ~ 2 - 4 X smaller $\Delta u'v'$ than CCFL, depending on the wavelength. This advantage is attributed to the narrower spectral bandwidth and less overlap of the RGB LED light sources.

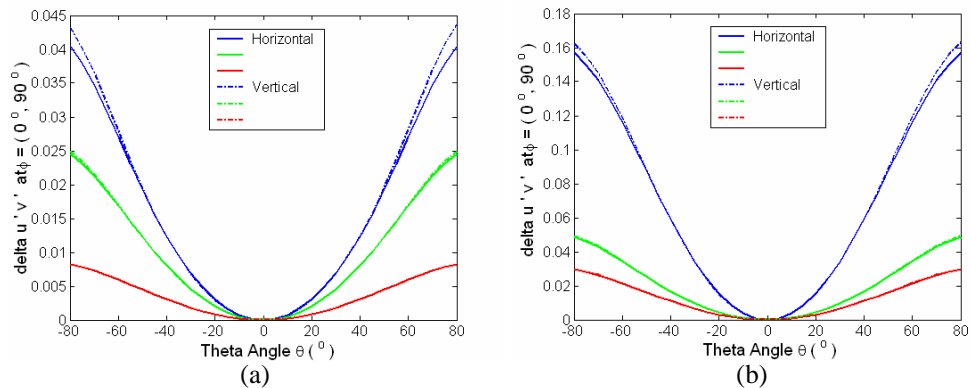


Fig. 8. Static color shift for RGB primaries in the horizontal and vertical directions. (a) LED and (b) CCFL.

4.6 Dynamic color shift between G63 and G255

Unlike computer monitors, in a TV the displayed images move frequently. Therefore, it is more important to evaluate the color uniformity between different gray levels (G63 and G255) than at a fixed gray level G255. Figure 9 plots the simulated dynamic color shifts of the IPS LCD between G63 and G255 gray levels along the horizontal direction ($\phi=0^\circ$) using the LED and CCFL backlights. Again, the RGB-LED backlight outperforms CCFL by a large margin. From Fig. 9, the dynamic color shift of the CCFL primaries between G63 and G255 levels are greatly reduced in comparison to the static color shift of G255 as Fig. 8(b) shows. In Fig. 9,

the $\Delta u'v'$ value is below 0.040 for the blue primary at $\theta = \pm 80^\circ$, and is lower than 0.010 and 0.004 for the green and red primaries, respectively. For the dynamic color shifts of the LED primaries shown in Fig. 9, its maximum $\Delta u'v'$ values are 0.0004, 0.0025 and 0.0122 at $\theta = \pm 80^\circ$ for the respective RGB primaries. These data are also improved as compared to those of the static color shifts plotted in Fig. 8(a). Small dynamic color shift helps to reduce the motion artifacts between the continuous frame images in different gray levels. Therefore, the RGB-LED backlight provides more vivid color images than CCFL in a LCD TV.

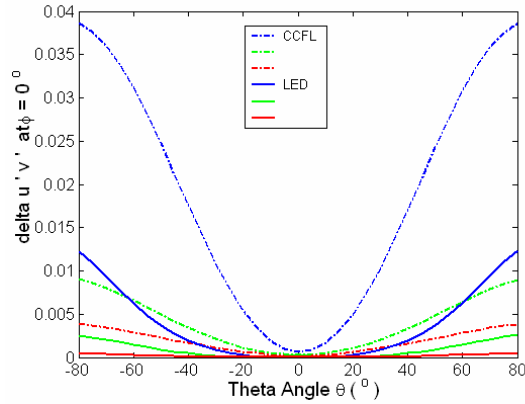


Fig. 9. Dynamic color shift comparison for different RGB primaries in the horizontal direction.

5. Conclusion

We have obtained quantitative results of the multi-domain IPS LCD using RGB LEDs and CCFL as a backlight unit. The LED system not only exhibits a wider color gamut but also has a 2-4X smaller color shift than CCFL in both static and dynamic color shifts. Wide spread applications of LED backlights for high-end LCD monitors and LCD TVs are foreseeable.

The authors are indebted to the financial support of Chi-Mei Optoelectronics Corporation (Taiwan).